# Long non-coding RNA SNHG16 functions as a tumor activator by sponging miR-373-3p to regulate the TGF-β-R2/SMAD pathway in prostate cancer

WUBIN WENG[1], CHANGMING LIU[1], GUOMIN LI[1], QIONGFANG RUAN[2], HUIZHANG LI[1], NINGFENG LIN[1] and GUANGBING CHEN[1]

[1]Department of Urology, Mindong Hospital Affiliated to Fujian Medical University; [2]Department of Respiratory Medicine, Mindong Hospital Affiliated to Fujian Medical University, Fuan, Fujian 355000, P.R. China

Received April 29, 2021; Accepted September 14, 2021

DOI: 10.3892/mmr.2021.12483

**Abstract.** Long non-coding RNAs (lncRNAs) are involved in the pathogenesis of prostate cancer (PCa) as competitive endogenous RNA. The present study aimed to investigate the molecular mechanisms of lncRNA small nucleolar RNA host gene 16 (SNHG16) in the proliferation and metastasis of PCa cells. Cancer tissues and adjacent normal tissues were collected from 80 patients with PCa who did not receive any treatment. Reverse transcription-quantitative PCR analysis was performed to detect the expression levels of SNHG16, hsa-microRNA (miRNA/miR)-373-3p and transforming growth factor-β receptor type 2 (TGF-β-R2), and Spearman's correlation coefficient analysis was performed to assess the correlations between these molecules. Furthermore, the effects of SNHG16 knockdown and overexpression on the biological functions of DU-145 PCa cells and TGF-β-R2/SMAD signaling were analyzed. The dual-luciferase reporter assay was performed to assess the associations between SNHG16 and miR-373-3p, and TGF-β-R2 and miR-373-3p, the effects of which were verified via rescue experiments. The results demonstrated that the expression levels of SNHG16 and TGF-β-R2 were significantly upregulated in PCa tissues, whereas miR-373-3p expression was significantly downregulated (P<0.001). In addition, negative correlations were observed between SNHG16 and miR-373-3p (rho, -0.631) and miR-373-3p and TGF-β-R2 (rho, -0.516). Overexpression of SNHG16 significantly promoted the proliferation, migration and invasion of PCa cells (P<0.05), and significantly increased the protein expression levels of TGF-β-R2, phosphorylated (p)-SMAD2, p-SMAD3, c-Myc and E2F4 (P<0.001). Notably, the results revealed that miR-373-3p is a target of SNHG16, and miR-373-3p knockdown rescued short hairpin (sh)-SNHG16-suppressed cellular functions by promoting TGF-β-R2/SMAD signaling. The results also revealed that miR-373-3p targets TGF-β-R2. Notably, transfection with miR-373-3p inhibitor rescued sh-TGF-β-R2-suppressed cell proliferation and migration. Taken together, the results of the present study suggest that SNHG16 promotes the proliferation and migration of PCa cells by targeting the miR-373-3p/TGF-β-R2/SMAD axis.

*Correspondence to:* Professor Changming Liu, Department of Urology, Mindong Hospital Affiliated to Fujian Medical University, 89 Heshan Street, Fuan, Fujian 355000, P.R. China
E-mail: mdyylcm@163.com

*Key words:* prostate cancer, long non-coding RNA small nucleolar RNA host gene 16, hsa-microRNA-373-3p, transforming growth factor-β receptor type 2/SMAD pathway, DU-145 cells

## Introduction

Incident cases of prostate cancer (PCa) have increased by 3.7-fold from 1990 to 2015, and the numbers continue to increase with an increase in screening popularity and life expectancy (1). PCa is the one of leading cause of cancer-associated mortality in men (2). In 2017, the number of newly diagnosed cases of PCa was 161,360, which was the first among the newly diagnosed cancer cases in men, accounting for 19% cancer cases, and the cases of death were 26,730, which was the third-leading cause of cancer-related mortality in men, accounting for 8% (3). By 2020, the new diagnoses of PCa increase to 191,930 cases, and the number of deaths was 33,330, becoming the second-leading cause of cancer-related mortality in men and aggravating the global burden of PCa (4). The development of disease severity increases genome changes and molecular complexity, thereby affecting PCa development and precision therapy (5). It is important to understand the carcinogenic effects and underlying mechanisms associated with PCa for accurate detection and to provide intervention approaches.

The role of non-coding RNA in the occurrence, progression and treatment of PCa has previously been reported (6). Long non-coding RNAs (lncRNAs) and microRNAs (miRNAs/miRs) are essential participants in the field of non-coding RNAs, and they have received great interest due to their abundance, specific expression, functional role in diseases and potential clinical applications (7). lncRNAs are >200 bases in length and transcribed from the genomic intergenic regions,

which regulate the expression of genes at epigenetic, transcriptional and post-transcriptional levels (8). For example, LINC00844 inhibits the progression and metastasis of PCa, whereas HOXD-AS1 and PCA3 promote tumor growth, castration resistance and chemoresistance (9-11). lncRNAs act as competitive endogenous RNA (ceRNA) to regulate miRNA expression (12,13). miRNAs are a type of small non-coding RNA, 17-22 nucleotides in length. Mature miRNAs suppress gene expression by recognizing the complementary target site in the 3'-untranslated region (UTR) of the target mRNA (14). miRNAs can also act as activators or inhibitors of cancer (15). According to reports, 19,075 lncRNA-miRNA-mRNA regulatory networks have been screened, and may be involved in the pathogenesis of PCa (16).

lncRNA small nucleolar RNA host gene 16 (SNHG16) is a novel oncogene identified in different types of cancer, such as colorectal cancer, hepatocellular carcinoma and glioma (17-20). A previous study has reported that SNHG16, which is upregulated in patients with PCa, can promote the expression of glucose transporter 1 and induce glucose uptake and cell proliferation (21). SNHG16 regulates glucose metabolism and participates in tumor lipid metabolism via ceRNA (17). Glucose and lipid metabolism are the major metabolic pathways of tumor cells (22). SNHG16 carcinogenic signal may be one of the ways for tumor cells to obtain energy (17,21,23). SNHG16 also acts as a ceRNA to drive vascular endothelial cell proliferation, migration, invasion and vasoformation by the modulating miR-520d-3p/STAT3 axis (24). Angiogenesis plays a key role in promoting tumor growth and metastasis (25). SNHG16 also promotes tumor proliferation and metastasis by directly targeting the miR-216A-5p/ZEB1 and miR-17-5p/p62 axes (18,19). SNHG16 is considered a central regulator in diverse biological processes controlling tumorigenesis, including promoting metabolic energy, growth, metastasis and chemoresistance (23). A recent study confirmed that SNHG16 is highly expressed in glioma, and regulates epidermal growth factor receptor by sponging miR-373-3p via the PI3K/AKT pathway to exert its carcinogenic function (20). In addition, miR-373-3p expression is downregulated by testicular nuclear receptor 4, which increases PCa cell invasion (26); thus, miR-373 may be a therapeutic target for PCa (27). In choriocarcinoma, upregulated miR-373-3p expression partly accounts for the downregulation of transforming growth factor-β receptor type 2 (TGF-β-R2), which suppresses epithelial-to-mesenchymal transition (EMT) and migration (28). Dysregulation of miR-373 has been reported in different types of cancer, and it is involved in nearly all cellular processes, acting as an oncogene or a tumor suppressor (29). For example, miR-373-3p is significantly upregulated in tongue squamous cell carcinoma tissues, and by directly targeting DKK1, it constitutively activates Wnt/β-catenin signaling, thereby promoting EMT-induced tumor metastasis (30). However, miR-373 is downregulated in lung cancer and acts as a tumor suppressor to attenuate cell proliferation, migration, invasion and mesenchymal phenotype by targeting interleukin 1 receptor associated kinase 2 and lysosomal associated membrane protein 1 (31).

TGF-β-R2 is a potential PCa suppressor (32). Deletion of TGF-β-R2 may increase the stemness capacity of PCa cells and cause rapid tumor development (33). The aberrant expression levels of lncRNAs and miRNAs, which contribute to cell proliferation, metastasis and drug resistance in PCa, are potential biomarkers and therapeutic targets (34). However, the role of the SNHG16/miR-373-3p signal axis in regulating the proliferation and metastasis of PCa cells remains unclear. Thus, the present study aimed to investigate the function of the SNHG16/miR-373-3p axis in the progression of PCa.

## Materials and methods

*Clinical tissue collection*. A total of 80 patients with PCa at the Mindong Hospital Affiliated to Fujian Medical University were enrolled in the present study between February 2019 and January 2020. PCa tumor tissues and paired adjacent normal tissues (2 cm away from the lesion) were collected by resection. All patients, without history of preoperative radiotherapy or chemotherapy, were confirmed to have PCa via analysis from three pathologists. The inclusion criteria were: i) Patients underwent surgical treatment; ii) pathologically diagnosed as PCa; and iii) no radiotherapy, chemotherapy and immunotherapy before surgery. Exclusion criteria were: i) Combined with other malignant tumors; ii) received radiotherapy and chemotherapy; iii) history of prostate surgery; and iv) blood system diseases. All specimens were immediately stored in liquid nitrogen at -80˚C until subsequent experimentation. The pathological type for all patients was adenocarcinoma. The clinicopathological characteristics of all patients, including age, tumor-node-metastasis (TNM) stage, International Society of Urological Pathology (ISUP) grade and serum prostate-specific antigen (sPSA) were recorded and analyzed to assess the associations between the *in vitro* findings and clinical presentations (35). The present study was approved by the Ethics Committee of Mindong Hospital Affiliated to Fujian Medical University [batch no. (2019) NingMin Medical Ethics approval no. (0110-1)], and performed in accordance with the Declaration of Helsinki. Written informed consent was provided by all patients prior to the study start.

*Cell culture*. The human PCa cell lines, DU-145 (HTB-81), PC-3 (CRL-1435), 22Rv-1 (CRL-2505) and LNCaP (CRL-1740), and the normal prostate epithelial cell line, RWPE1 (CRL-11609) were purchased from the American Type Culture Collection. DU-145, 22Rv-1 and LNCaP cells were maintained in RPMI-1640 medium (Gibco; Thermo Fisher Scientific, Inc.). PC-3 cells were cultured in F-12K medium (American Type Culture Collection). PCa cells were maintained in RPMI-1640 or F-12K medium supplemented with 10% fetal bovine serum (PAN Biotech Ltd.), 4 mM L-glutamine (MedChemExpress), 100 U/ml penicillin (MedChemExpress) and 100 $\mu$g/ml streptomycin (MedChemExpress). RWPE1 cells were cultured in keratinocyte serum-free medium (Gibco; Thermo Fisher Scientific, Inc.), and the medium included 0.05 mg/ml extractive from bovine pituitary and 5 ng/ml human recombinant epidermal growth factor. All cells were incubated at 37˚C in a humidified atmosphere of 5% $CO_2$.

*Reverse transcription-quantitative (RT-q)PCR*. Total RNA was extracted from PCa tissues and cells using NucleoZOL® (Gene Co., Ltd.; https://www.genetech.com.cn/). Total RNA (10 $\mu$g) was reverse transcribed into cDNA using the RT System kit

(Takara Bio, Inc.) and PCR instrument (Heal Force; http://www.healforce.com/cn/). The reaction conditions were as follows: 25˚C for 5 min, 42˚C for 60 min and 75˚C for 15 min. The primer sequences used for qPCR were designed and synthesized by Shanghai GenePharma Co., Ltd. The primer sequences were resuspended in 250 $\mu$l RNase-free water to a final concentration of 10 $\mu$M. qPCR reaction was subsequently performed using 12.5 $\mu$l SYBR-Green qPCR Master Mix (Takara Bio, Inc.), 1 $\mu$l upstream and downstream primers, 2 $\mu$l RT product and 8.5 $\mu$l RNase free water. The following thermocycling conditions were used: 40 PCR amplification cycles were performed with initial incubation at 95˚C for 10 min and final extension at 72˚C for 5 min. Each cycle comprised denaturation at 95˚C for 10 sec, annealing at 60˚C for 30 sec and extension at 72˚C for 30 sec. The following primer sequences were used for qPCR: SNHG16 forward, 5'-GTGCCTCAGGAAGTCTTGCC-3' and reverse, 5'-ATCCAAACAAGTTATCAGCAGCAGCAC-3'; TGF-β-R2 forward, 5'-GTAGCTCTGATGAGTGCAATGAC-3' and reverse, 5'-CAGATATGGCAACTCCCAGTG-3'; miR-373-3p forward, 5'-GCGGAAGTGCTTCGATTTTG-3' and reverse, 5'-AGTGCAGGGTCCGAGGTATT-3'; RT primer, 5'-GTCGTATCCAGTGCAGGGTCCGAGGTATTCGCACTGGATACGACACACCC-3'; GAPDH forward, 5'-CACCCACTCCTCCACCTTTGA-3' and reverse, 5'-TCTCTCTTCCTCTTGTGCTCTTGC-3'; U6 forward, 5'-CTCGCTTCGGCAGCACATATACT-3' and reverse, 5'-ACGCTTCACGAATTTGCGTGTC-3'; and RT primer, 5'-AAAATATGGAACGCTTCACGAATTTG-3'. Relative expression levels were calculated using the $2^{-\Delta\Delta Cq}$ method (36). SNHG16 and TGF-β-R2 were normalized to the internal reference gene GAPDH, while miR-373-3p expression was normalized to U6.

*Cell transfection*. Prior to transfection, DU-145 cells were seeded into 24-well plates at a density of $1x10^5$ cells/well. Lipofectamine® 2000 (Invitrogen; Thermo Fisher Scientific, Inc.) was used for cell transfection. For SNHG16 gene knockdown experiments, short hairpin (sh)RNA was amplified using the following primer sequences: shRNA-SNHG16, 5'-GATCCGGATGAGACTTAACTTAAATTCAAGAGATTTAAGTTAAGTCTCATCCTTTTTG-3', and shRNA-negative control (NC), 5'-GATCCGTGTAGATGCGTTGTGATATTCAAGAGATATCACAACGCATCTACACTTTTTG-3' (Thermo Fisher Scientific, Inc.). The product was subsequently digested using *Bam*hI and *Eco*RI restriction enzymes (Fermentas; Thermo Fisher Scientific, Inc.), and the fragment was inserted into the *Bam*hI/*Eco*RI sites of the pLVX-shRNA2-Puro vector (Zolgene Biotechnology Co., Ltd., http://www.zolgene.com/). For SNHG16 overexpression, cells were transfected with SNHG16 overexpression construct (pcDNA3.1-SNHG16) (Zolgene Biotechnology Co., Ltd.), and the NC was a pcDNA3.1 vector (Invitrogen; Thermo Fisher Scientific, Inc.). Specifically, the full length of SNHG16 was obtained via PCR amplification using the following primer sequences: SNHG16 forward, 5'-CGGGATCCCGGCGTTCTTTTCGAGGTCGGCCG-3' and reverse, 5'-CCCTCGAGGGTGACGGTAGTTTCCCAAGTTTA-3'. The amplified product was subsequently digested using *Bam*hI and *Xho*I restriction enzymes, and the fragment was inserted into the BamhI/XhoI sites of the pcDNA3.1 vector to obtain the SNHG16 overexpression plasmid. When the DU-145 cells reached 30-50% confluence, 10 nM pLVX-shRNA2-Puro-NC, pLVX-shRNA2-Puro-SNHG16, pcDNA3.1 and pcDNA3.1-SNHG16 plasmids were used to transfect cell at 37˚C for 48 h.

Next, miR-373-3p mimic, inhibitor and the respective NCs were purchased from Shanghai GenePharma, Co., Ltd. The following primer sequences were used: miR-373-3p mimic, 5'-GAAGUGCUUCGAUUUUGGGGUGU-3'; mimic NC, 5'-UCACAACCUCCUAGAAAGAGUAGA-3'; miR-373-3p inhibitor, 5'-ACACCCCAAAAUCGAAGCACUUC-3'; and inhibitor NC, 5'-UCUACUCUUUCUAGGAGGUUGUGA-3'. When the DU-145 cells reached 30-50% confluence, 10 nM miR-373-3p mimic, inhibitor and the NC were used to transfect cells, which were cultured in a 5% $CO_2$ incubator at 37˚C for 48 h. After confirming the transfection efficiency of miR-373-3p mimic and inhibitor, pLVX-shRNA2-Puro-SNHG16-NC (10 nM) and miR-373-3p inhibitor NC (10 nM), pLVX-shRNA2-Puro-SNHG16 (10 nM), miR-373-3p inhibitor (10 nM), pLVX-shRNA2-Puro-SNHG16 (10 nM) and miR-373-3p inhibitor (10 nM) plasmids were used to transfect DU-145 cell for 48 h at 37˚C in an incubator (SANYO Trading Co., Ltd.; https://www.sanyo-si.com/).

Third, The shRNA and shRNA-NC sequences targeting TGF-β-R2 were synthesized by Shanghai Sangon Biotech, Co., Ltd. The shRNA targeting TGF-β-R2 was 5'-GGTGGGAACTGCAAGATACATCTGTGCTGTCCATGTATCTTGCAGTTCCCACCTTTTT-3', and the shRNA-NC was 5'-GATCCGATCAATACTATTCATCAATTCAAGAGATTGATGAATAGTATTGATCTTTTTG-3'. The pLVX-shRNA2-Puro vector, *Eco*RI and *Bam*hI were used to construct the TGF-β-R2 knockdown and NC plasmids. Then, miR-373-3p inhibitor NC (10 nM) and pLVX-shRNA2-Puro-TGF-β-R2-NC (10 nM), pLVX-shRNA2-Puro-TGF-β-R2 (10 nM), miR-373-3p inhibitor (10 nM), pLVX-shRNA2-Puro-TGF-β-R2 (10 nM) and miR-373-3p inhibitor (10 nM) were used for transfection at 37˚C when the DU-145 cells reached 30-50% confluence. Subsequent experiments were performed 48 h post-transfection. The experiments were performed in triplicate.

*Cell Counting Kit-8 (CCK-8) assay*. Cell proliferation was assessed via the CCK-8 assay (Dojindo Laboratories, Inc.). DU-145 cell suspensions were transferred into 96-well plates at a density of $1x10^4$ cells/ml and incubated for 24, 48, 72 and 96 h at 37˚C. Subsequently, 10 $\mu$l of CCK-8 reagent was added to each well and further incubated for 4 h. Absorbance was measured at a wavelength of 450 nm, using a microplate reader (Perlong; https://ziyeyl.chemdrug.com/sell/).

*Apoptosis analysis*. Cells were seeded into 24-well plates at a density of $1x10^5$ cells/well and transfected until they reached 60-70% confluence. After transfecting with plasmid for 48 h, cells were washed twice with PBS and centrifuged at room temperature and 220 x g for 5 min. Cells were subsequently incubated with 5 $\mu$l of Annexin V-FITC for 15 min and 10 $\mu$l of PI for 5 min at room temperature, in the dark (BD Biosciences), according to the manufacturer's instructions. Apoptotic cells were subsequently analyzed via flow cytometry (Becton-Dickinson and Company).

*Gap closure assay*. Cell migration was assessed via the gap closure assay. Following transfection with plasmid for 48 h, cells were seeded into both sides of the Ibidi-cell

plug-in (Corning, Inc.) in 24-well plates at a density of 3x105 cells/well. After 24 h of cell culture, the Ibili-cell plug-in was removed and the culture in serum-free medium was continued. Following incubation for 24 h at 37˚C, cells were observed under a florescence microscope at x100 magnification (Mshot; http://www.mshot.com.cn/). The gap closure migrated area was measured using ImageJ software (version number, 1.42; National Institutes of Health). The formula used was: Gap closure area (%) = (0 h area-24 h area)/0 h area x100%.

*Transwell assay*. Cell invasion was assessed using a Transwell chamber (8 $\mu$m pore size, Corning, Inc.) deposited with Matrigel (BD Biosciences). The melted Martrigel in a 4˚C refrigerator was diluted in serum-free medium at 1:8. Then, 50 $\mu$l diluted Martrigel was used to coat the upper chamber of Transwell, which was air dried at 4˚C and solidify at 37˚C for 30 min. Following transfection with plasmid for 48 h, cells were resuspended in serum-free medium and seeded in the upper chamber with $1x10^5$ cells, while complete media (RPMI-1640 medium with 10% fetal bovine serum, 4 mM L-glutamine, 100 U/ml penicillin and 100 $\mu$g/ml streptomycin) was plated in the lower chamber. Following incubation for 24 h at 37˚C, cells in the upper membrane were removed. At room temperature, the invasive cells were fixed with 4% paraformaldehyde for 30 min, stained with 0.1% crystal violet for 15 min and observed under the florescence microscope at x100 magnification (MSHOT; http://www.mshot.com.cn/mf52.htm).

*Western blotting*. Following transfection for 48 h, DU-145 cells were collected by centrifuging at 220 x g room temperature for 5 min. RIPA buffer (Takara Bio, Inc,) and protease inhibitor [Roche Diagnostics (Shanghai) Co., Ltd.] were used for cell lysis. The BCA assay kit was used to detect protein concentration (Epizyme, Inc.). Then, 10 $\mu$l protein samples were separated via 10% SDS-PAGE, transferred onto PVDF membranes and blocked with 5% skim milk in 20 mM Tris-HCl, 150 mM NaCl, 0.1% Tween-20 for 1 h at room temperature The membranes were incubated with primary antibodies against TGF-β-R2 (cat. no. 41896, 85 kDa), c-Myc (cat. no. 18583, 65 kDa), E2F4 (cat. no. 40291, 62 kDa), SMAD2 (cat. no. 5339, 60 kDa), phosphorylated (p)-SMAD2 (cat. no. 3108, 60 kDa), SMAD3 (cat. no. 9523, 52 kDa), p-SMAD3 (cat. no. 9520, 52 kDa) and β-actin (cat. no. 4970, 45 kDa) overnight at 4˚C (all 1:1,000 and Cell Signaling Technology, Inc.). The membranes were washed twice with PBS and subsequently incubated with HRP-conjugated Affinipure Goat Anti-Rabbit IgG(H+L) (ProteinTech Group, Inc., 1:5,000, cat. no. SA00001-2) for 2 h at room temperature. Protein bands were visualized using ECL Western blotting reagents (Cytiva), imaged using Tanon 5200 Biotanon (Tanon Science & Technology Co., Ltd.) and analyzed using ImageJ software (version number, 1.42; National Institutes of Health).

*Dual-luciferase reporter assay*. According to TargetScan (http://www.targetscan.org/vert_72/, version number, 7.2) and StarBase (http://starbase.sysu.edu.cn/, version no. 2.0) databases, the fragments from SNHG16 and TGF-β-R2 containing the predicted miR-373-3p binding sites and its mutant (MUT) sequence were directly synthesized (Table SI). The sequences of SNHG16-3'-UTR-wild-type (WT), SNHG16-3'-UTR-MUT, TGF-β-R2 3'-UTR-WT and TGF-β-R2 3'-UTR-MUT were synthesized by Shanghai, GenePharma, Co., Ltd., and digested using *Xho*I and *Not*I restriction enzymes (Fermentas; Thermo Fisher Scientific, Inc.). The 3'-UTR fragments were subsequently inserted into the *Xho*I/*Not*I sites of the psiCHECK-2 vector (Promega Corporation) to obtain luciferase reporter plasmids.

DU-145 cell suspensions were seeded into 24-well plates at a density of 1x105 cells/well and incubated for 24 h at 37˚C. The psiCHECK-2-SNHG16-WT or psiCHECK-2-SNHG16-MUT (Zolgene Biotechnology Co., Ltd.; http://www.zolgene.com/) reporter plasmids (20 ng) were co-transfected with miR-373-3p mimics or mimic NC (10 nM) into cells, using Lipofectamine® 2000 (Invitrogen; Thermo Fisher Scientific, Inc.) to verify the targeting effect of SNHG16 and miR-373-3p. Similarly, the psiCHECK-2-TGF-β-R2-WT or psiCHECK-2-TGF-β-R2-MUT reporter plasmids (Zolgene Biotechnology Co., Ltd.; http://www.zolgene.com/) (20 ng) were co-transfected with miR-373-3p mimics or mimic NC (10 nM) into cells, using Lipofectamine® 2000 to verify the targeting effect of TGF-β-R2 and miR-373-3p. Following transfection for 36 h at 37˚C, cell lysates were prepared using lysis buffer (Promega Corporation). Firefly and *Renilla* luciferase activities were detected via the dual-luciferase reporter assay (Promega Corporation). *Renilla* luciferase values were divided by the Firefly luciferase values to normalize the difference in transfection efficiency.

*Statistical analysis*. Statistical analysis was performed using SPSS 20.0 software (IBM Corp.). The experiment was repeated three times, and data were presented as the mean ± SD. If the data followed the normal distribution, Student's t-test was used for pairwise comparison, and one-way ANOVA followed by Tukey's post hoc test was used to compare differences between multiple groups. If the data did not follow the normal distribution, Wilcoxon signed-rank test was used for paired data, while Mann-Whitney U test was used for unpaired data. Spearman's correlation coefficient analysis was performed to assess the correlation between SNHG16 and miR-373-3p, and TGF-β-R2 and miR-373-3p. Patients with PCa were divided into high expression group (n=40) and low expression group (n=40) based on the median expression of SNHG16, miR-373-3p and TGF-β-R2. Then, Pearson's $\chi^2$ test and Fisher's exact test were used for descriptive analysis. $P<0.05$ was considered to indicate a statistically significant difference.

## Results

*Correlation between the expression levels of SNHG16, miR-373-3p and TGF-β-R2 and the clinicopathological characteristics of patients with PCa*. Patient characteristics are presented in Table I. According to SNHG16 expression, 80 cases of PCa tissues were divided into: Low SNHG16 expression (below the median SNHG16 expression, n=40), and high SNHG16 expression (above the median SNHG16 expression, n=40) groups. According to miR-373-3p expression, PCa tissues were divided into: Low miR-373-3p expression (below the median, n=40), and high miR-373-3p expression (above the median, n=40) groups. Grouping according to TGF-β-R2 gene expression: Low TGF-β-R2 expression (below the median, n=40) and high TGF-β-R2 expression (above the median, n=40) groups. The expression levels of SNHG16,

Table I. Correlation between the expression levels of SNHG16, hsa-miR-373-3p and TGF-β-R2 and the clinicopathological characteristics of patients with prostate cancer (n=80).

| | | | SNHG16 expression | | | miR-373-3p expression | | | TGF-β-R2 expression | |
|---|---|---|---|---|---|---|---|---|---|---|
| Characteristics | Cases, n (%) | P-value | Low, n | High, n | P-value | Low, n | High, n | P-value | Low, n | High, n |
| Age, years | | | | | | | | | | |
| <60 | 55 (68.75) | 28 | 27 | 0.809 | 26 | 29 | 0.469 | 29 | 26 | 0.469 |
| ≥60 | 25 (31.25) | 12 | 13 | | 14 | 11 | | 11 | 14 | |
| ISUP grade | | | | | | | | | | |
| ≤3 | 41 (51.25) | 25 | 16 | 0.044[a] | 14 | 27 | 0.004[b] | 29 | 12 | <0.001[c] |
| ≥4 | 39 (48.75) | 15 | 24 | | 26 | 13 | | 11 | 28 | |
| TNM stage | | | | | | | | | | |
| ≤T2 | 53 (66.25) | 25 | 28 | 0.478 | 27 | 26 | 0.813 | 25 | 28 | 0.478 |
| ≥T3 | 27 (33.75) | 15 | 12 | | 13 | 14 | | 15 | 12 | |
| sPSA, ng/ml | | | | | | | | | | |
| <20 | 11 (13.75) | 7 | 4 | 0.518 | 3 | 8 | 0.193 | 8 | 3 | 0.193 |
| ≥20 | 69 (86.25) | 33 | 36 | | 37 | 32 | | 32 | 37 | |

[a]P<0.05; [b]P<0.01; [c]P<0.001. Data are presented as numbers and percentages. Analysis was performed using (a) Pearson's $\chi^2$ test (age, ISUP grade and TNM stage), and (b) Fisher's exact test (sPSA). ISUP, International Society of Urological Pathology; TNM, tumor-node-metastasis; sPSA, serum prostate-specific antigen.

miR-373-3p and TGF-β-R2 had no significant correlations with age (<60 vs. ≥60 years), TNM stage (≤T2 vs. ≥T3) and sPSA (<20 vs. ≥20 ng/ml) (all P>0.05). However, the expression levels of SNHG16, miR-373-3p and TGF-β-R2 were significantly correlated with ISUP grade (≤3 vs. ≥4; P=0.044, P=0.004 and P<0.001, respectively).

*High SNHG16 expression promotes PCa development by regulating the TGF-β-R2/SMAD signaling pathway*. SNHG16 expression was significantly upregulated in PCa tissues compared with adjacent normal tissues (P<0.001; Fig. 1A). Similarly, SNHG16 and TGF-β-R2 expression levels were upregulated in DU-145 and PC-3 cells compared with RWPE1 cells. However, no significant differences in expression levels were observed in 22Rv-1 and LNCaP cells (P>0.05; Fig. S1A). Notably, miR-373-3p expression was significantly downregulated in DU-145 and PC-3 cells compared with RWPE1 cells (P<0.05; Fig. S1A). Thus, SNHG16 expression was knocked down and overexpressed in DU-145 cells. The expression of SNHG16 in the knockdown group was significantly lower than that in the sh-NC group, and in the overexpression group it was significantly increased compared with oe-NC group (P<0.01; Fig. 1B). The results demonstrated that overexpression of SNHG16 significantly promoted cell proliferation (P<0.001; Fig. 1C), invasion (P<0.05; Fig. 1E) and gap closure (P<0.001; Fig. 1F). However, overexpression of SNHG16 significantly inhibited cell apoptosis (P<0.01; Figs. 1D and S1B). Western blot analysis demonstrated that overexpression of SNHG16 significantly increased the protein expression levels of c-Myc, TGFBR2, E2F4, p-SMAD2/SMAD2 and p-SMAD3/SMAD3, the effects of which were reversed following SNHG16 knockdown (P<0.001; Fig. 1G).

*SNHG16 acts as miR-373-3p sponge to affect DU-145 cell biological processes by regulating TGF-β-R2/SMAD signaling*. TargetScan and StarBase analyses revealed that a binding site exists between SNHG16 and miR-373-3p (Fig. 2A). miR-373-3p expression was significantly downregulated in PCa tissues compared with adjacent normal tissues (P<0.001; Fig. 2B), and was negatively correlated with SNHG16 expression (rho, -0.631; P<0.001; Fig. 2C). DU-145 cells were transfected with miR-373-3p mimics and inhibitor. The expression of miR-373-3p in mimic group was significantly increased than NC group, while it was significantly decreased in inhibitor group. (P<0.001; Fig. 2D). The results of the dual-luciferase reporter assay revealed that miR-373-3p mimic transfection caused a significant reduction in the luciferase activity of SNHG16-WT (P<0.01), but not of SNHG16-MUT (P>0.05; Fig. 2E). Thus, SNHG16 showed biological binding to miR-373-3p. In addition, SNHG16 knockdown significantly increased miR-373-3p expression, the effects of which were reversed following transfection with miR-373-3p inhibitor (P<0.05; Fig. 2F).

The results demonstrated that transfection with miR-373-3p inhibitor significantly improved cell proliferation (P<0.001; Fig. 2G), and rescued invasion (P<0.01; Fig. 2I) and migration (P<0.01; Fig. 2J) inhibited by sh-SNHG16, and decreased sh-SNHG16-induced apoptosis (P<0.01; Figs. 2H and S1C). In addition, transfection with miR-373-3p inhibitor significantly increased the protein expression levels of c-Myc, TGFBR2, E2F4, p-SMAD2/SMAD2 and p-SMAD3/SMAD3 (P<0.001), and rescued the inhibition of sh-SNHG16 (Fig. 2K).

*miR-373-3p targets TGF-β-R2 to mediate DU-145 cell biological processes*. The binding site between miR-373-3p and TGF-β-R2 is presented in Fig. 3A. TGF-β-R2 mRNA

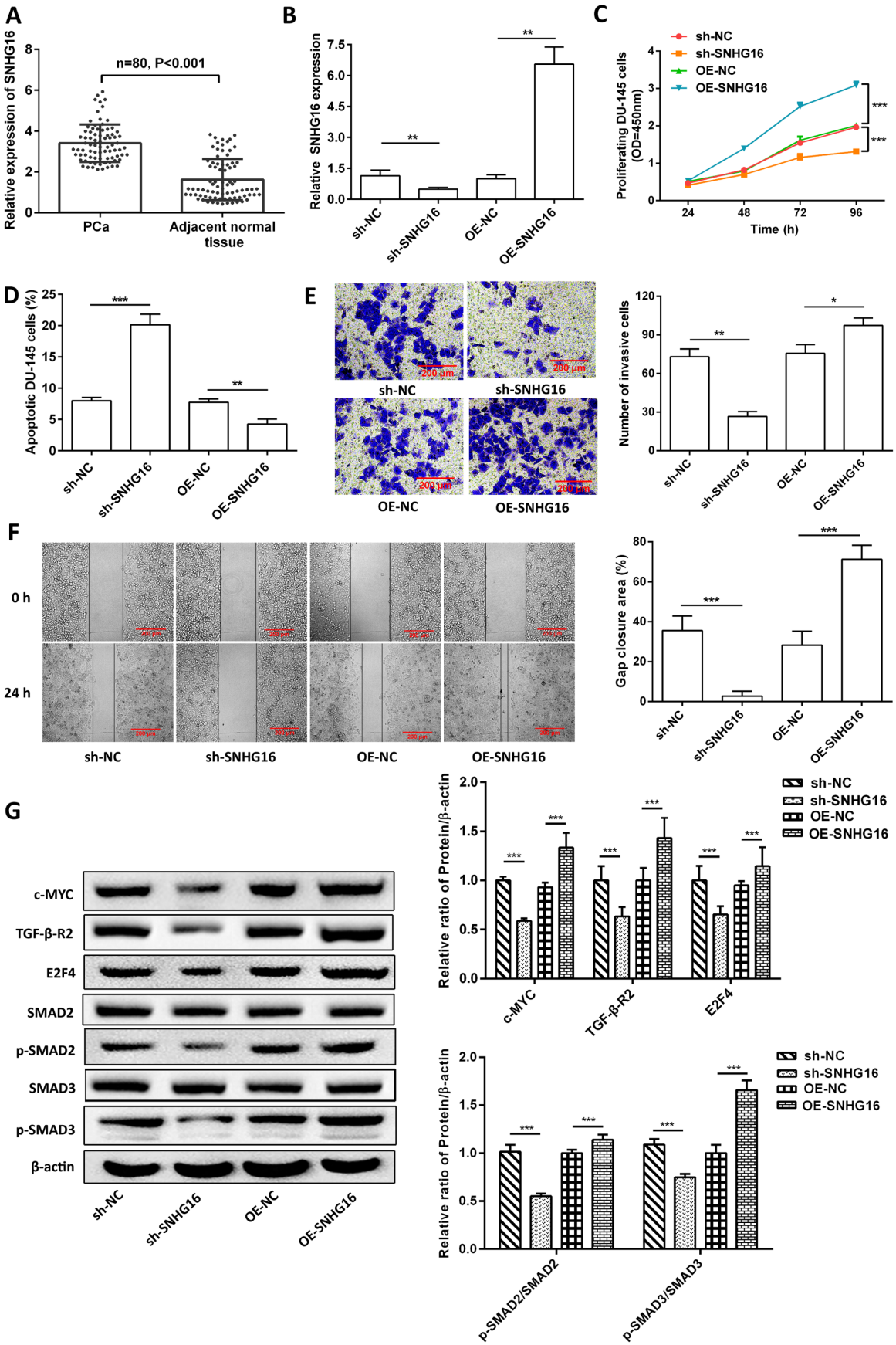


Figure 1. SNHG16 promotes the tumor process by regulating TGF-β-R2/SMAD signaling. (A) Reverse transcription-quantitative PCR analysis was performed to detect SNHG16 expression in PCa tissues and adjacent normal tissues. (B) SNHG16 expression was detected following knockdown or overexpression of SNHG16 in DU-145 cells. SNHG16 regulated (C) cell proliferation, (D) apoptosis, (E) invasion and (F) migration. (G) Western blot analysis was performed to detect the protein expression levels of c-Myc, TGF-β-R2, E2F4, SMAD2, p-SMAD2, SMAD3 and p-SMAD3. Data are presented as the mean ± SD (n=3). $^{*}$P<0.05; $^{**}$P<0.01; $^{***}$P<0.001. SNHG16, small nucleolar RNA host gene 16; TGF-β-R2, transforming growth factor-β receptor type 2; PCa, prostate cancer; p, phosphorylated; sh, short hairpin; NC, negative control; OE, overexpression; OD, optical density; lncRNA, long non-coding RNA.

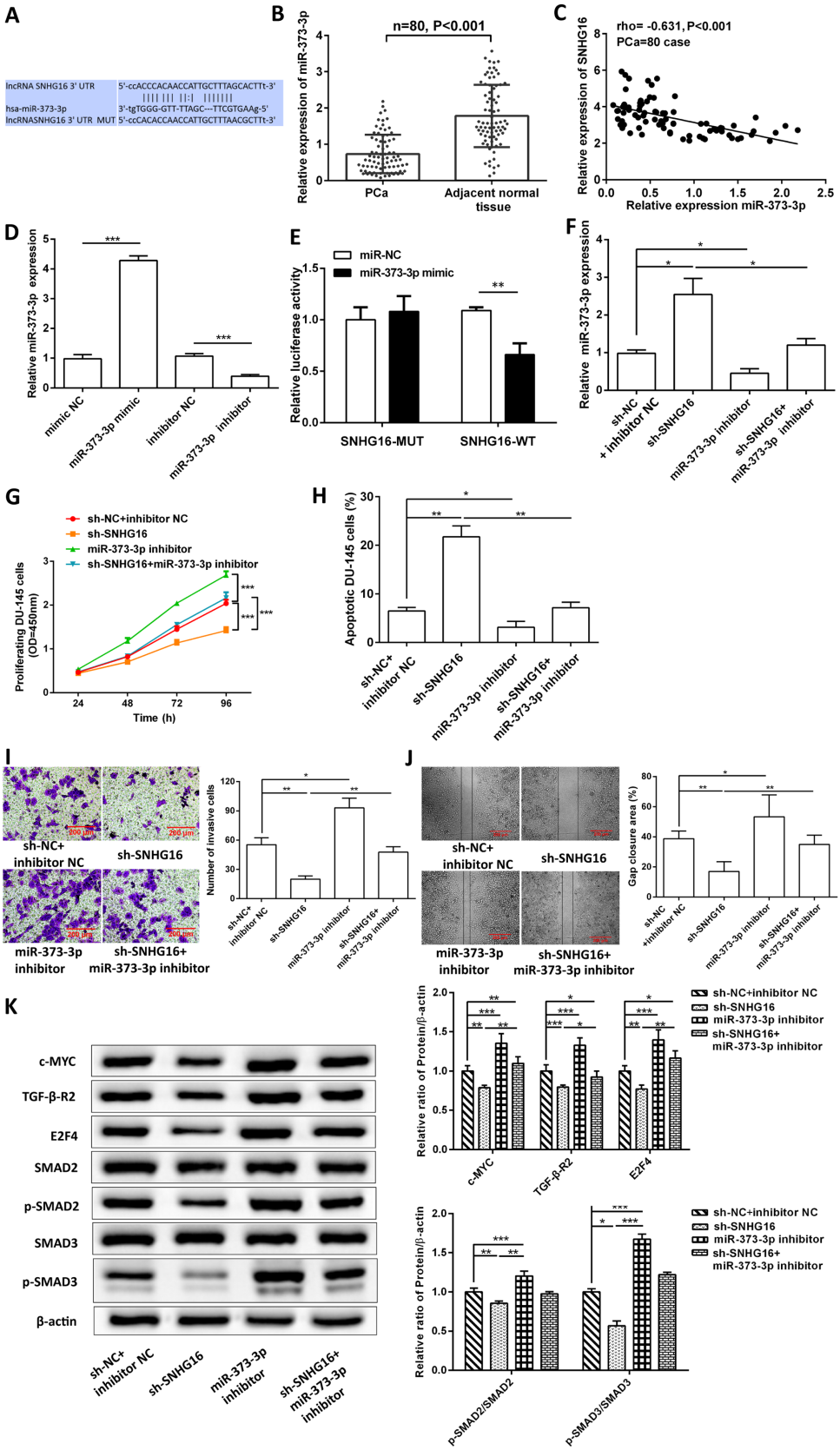


Figure 2. SNHG16 acts as a miR-373-3p sponge to affect DU-145 cell biological processes by regulating TGF-β-R2/SMAD signaling. (A) Binding sites between SNHG16 and miR-373-3p. (B) Reverse transcription-quantitative PCR analysis was performed to detect miR-373-3p expression in PCa tissues and adjacent normal tissues. (C) Spearman's correlation coefficient analysis was performed to assess the correlation between SNHG16 and miR-373-3p. (D) miR-373-3p expression was detected following overexpression or knockdown of miR-373-3p. (E) The dual-luciferase reporter assay was performed to verify the interaction between miR-373-3p and SNHG16. Transfection with miR-373-3p inhibitor partially reversed sh-SNHG16-regulated (F) miR-373-3p expression, (G) cell proliferation, (H) apoptosis, (I) invasion and (J) migration. (K) Western blot analysis was performed to detect the protein expression levels of c-Myc, TGF-β-R2, E2F4, SMAD2, p-SMAD2, SMAD3 and p-SMAD3. Data are presented as the mean ± SD (n=3). $^{*}$P<0.05; $^{**}$P<0.01; $^{***}$P<0.001. SNHG16, small nucleolar RNA host gene 16; miR, microRNA; PCa, prostate cancer; TGF-β-R2, transforming growth factor-β receptor type 2; sh, short hairpin; p, phosphorylated; N, negative control; MUT, mutant, WT, wild-type; OD, optical density.

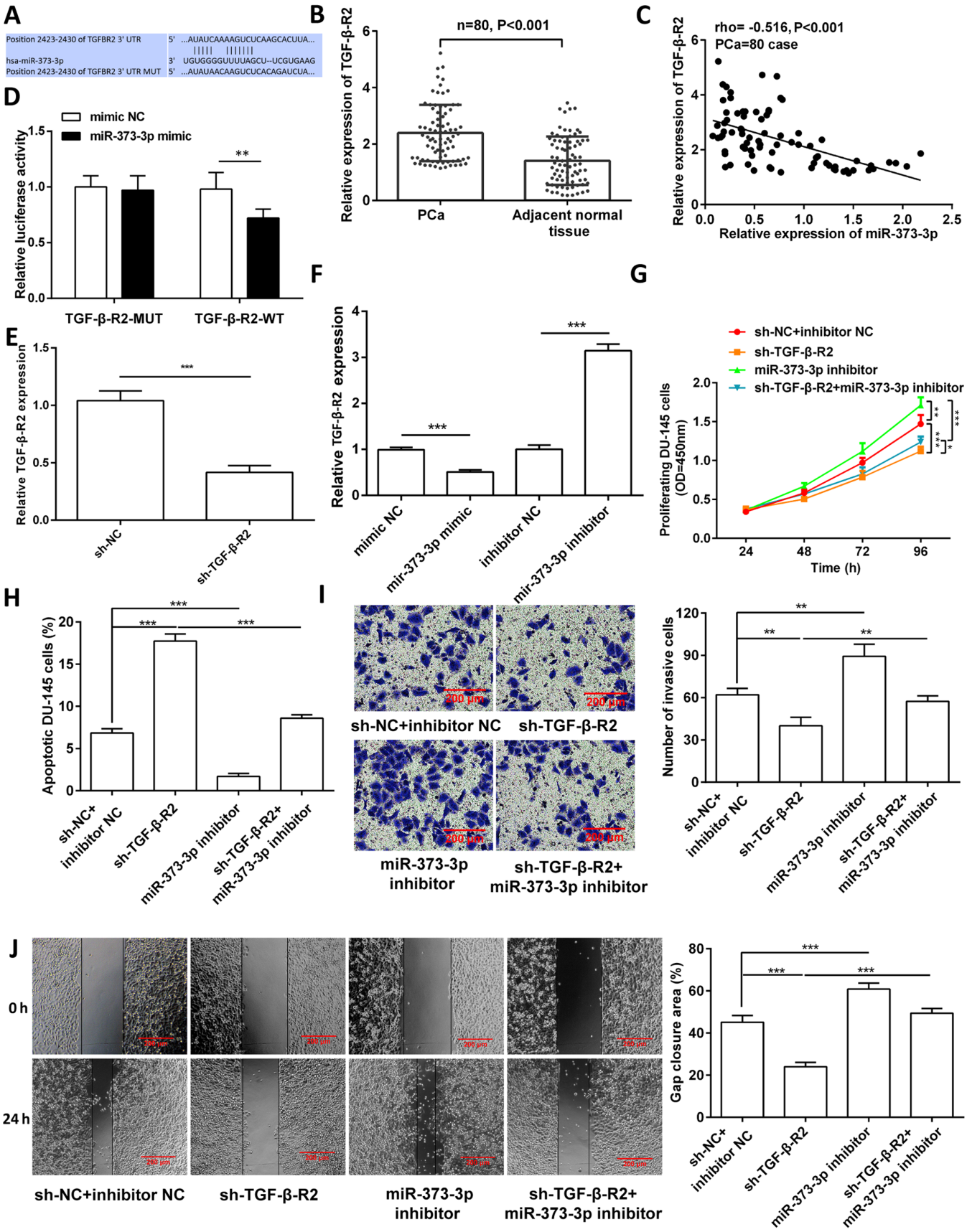


Figure 3. miR-373-3p targets TGF-β-R2 to mediate DU-145 cell biological processes. (A) Binding sites between miR-373-3p and TGF-β-R2. (B) Reverse transcription-quantitative PCR analysis was performed to detect TGF-β-R2 expression in PCa tissues and adjacent normal tissues. (C) Spearman's correlation coefficient analysis was performed to assess the correlation between TGF-β-R2 and miR-373-3p. (D) The dual-luciferase reporter assay was performed to verify the interaction between TGF-β-R2 and miR-373-3p. (E) TGF-β-R2 knockdown in DU-145 cells. (F) TGF-β-R2 expression was detected following overexpression or knockdown of miR-373-3p. TGF-β-R2 knockdown partially reversed the effects of miR-373-3p inhibitor-regulated (G) cell proliferation, (H) apoptosis, (I) invasion and (J) migration. Data are presented as the mean ± SD (n=3). $^{**}$P<0.01; $^{***}$P<0.001. miR, microRNA; TGF-β-R2, transforming growth factor-β receptor type 2; PCa, prostate cancer; NC, negative control; MUT, mutant; WT, wild-type; sh, short hairpin; OD, optical density.

expression was significantly upregulated in PCa tissues (P<0.001; Fig. 3B), and was negatively correlated with miR-373-3p expression (rho, -0.516; P<0.001; Fig. 3C). Luciferase activity was significantly reduced in the miR-373-3p mimic and TGF-β-R2-WT co-transfection group (P<0.001), but not after TGF-β-R2-MUT co-transfection (P>0.05; Fig. 3D). miR-373-3p showed biological binding to TGF-β-R2. TGF-β-R2 expression was knocked down in DU-145 cells (Fig. 3E). Notably, overexpression of miR-373-3p significantly decreased TGF-β-R2 mRNA expression (P<0.001; Fig. 3F). miR-373-3p inhibitor partially reversed the effects of TGF-β-R2 knockdown on cell proliferation (P<0.05; Fig. 3G), invasion (P<0.01; Fig. 3I) and migration (P<0.001; Fig. 3J), and increased miR-373-3p-inhibitor-suppressed apoptosis (P<0.001; Figs. 3H and S1D).

## Discussion

lncRNAs can function as modulators of biological processes, and act as oncogenes or tumor suppressor genes in PCa (9-11,37). The results of the present study confirmed that lncRNA SNHG16 is highly expressed in PCa. It also acted as a ceRNA to target modulation of miR-373-3p/TGF-β-R2/SMAD signaling, and exerted a carcinogenic effect. Previous studies have also shown that SNHG16 was upregulated in PCa tissues and promoted tumor proliferation (21), and that it exerted a carcinogenic function by sponging miR-373-3p in glioma (20). miR-373 was decreased in PCa (27), and targeting TGF-β-R2/p-SMAD3 signals inhibited PCa cell invasion and migration (26). To summarize, the current results were consistent with those of previous research.

SNHG16 has been reported to act as a tumor activator in neuroblastoma (38). The results of the present study demonstrated that SNHG16 was abnormally expressed at high levels in PCa. SNHG16 also promoted tumor cell proliferation, migration and invasion. High SNHG16 expression induces PCa cell proliferation by promoting glucose metabolism (21). SNHG16 is also a prognostic indicator of gastric cancer, and its overexpression is significantly associated with tumor invasion depth, lymph node metastasis, TNM stage and histological differentiation (39). In ovarian cancer cell lines, overexpression of SNHG16 is essential for tumor diagnosis and development (40). SNHG16 expression is upregulated in several malignancies and associated with tumor cell lines (41). However, reports of SNHG16 expression in colorectal cancer and hepatocellular carcinoma were conflicting (42,43). High-quality RNA and tumor cell specific gravity may explain the inconsistencies of SNHG16 expression (17). The results of the present study confirmed the oncogenic effect of SNHG16 in PCa cells. Notably, SNHG16 promoted PCa cell proliferation by regulating TGF-β-R2/SMAD signaling. Furthermore, SNHG16 upregulated TGF-β-R2 expression and promoted PCa cell viability. TGF-β-R2/SMAD signaling plays a crucial role in regulating the proliferation, differentiation and metastasis of PCa cells (32). TGF-β-R2 promotes EMT, migration and invasion of PCa cells (44,45).

SMAD2/3 interacts with PKCε, causing SMAD3 to bind to the promoter of glycolysis genes, inducing glycolysis gene expression and promoting aerobic glycolysis and PCa cell proliferation (46). However, SMAD3 or TGF-β-R2 significantly reduce the mass and microvascular density of PCa xenograft tumors (47). In addition, SMAD2/3 activates Rb/E2F4 and upregulates survivin to induce PCa progression and chemotherapy resistance (48). E2F4, which were upregulated in PCa cells, promotes cell cycle by forming complexes with P130 (49,50). c-Myc, a proto-oncogene, plays a key role in cell cycle progression, apoptosis and cellular transformation (51). Cancer stem cell-derived exosome-SNHG16 promotes cancer progression by activating TLR7/MyD88/NF-κB/c-Myc signaling (52). High c-Myc expression can promote PCa development by inducing the transcription of the androgen receptor gene (53). Taken together, these findings suggest that SNHG16 increases the expression levels of c-Myc, TGF-β-R2, E2F4, p-SMAD2 and p-SMAD3, and this development is an essential mechanism for its carcinogenic effects.

Increasing evidence suggest that SNHG16 can function as a ceRNA by sequestering miR-373-3p in glioma (20). The results of the present study demonstrated that low miR-373-3p expression was negatively correlated with SNHG16, and SNHG16 acted as a miR-373-3p sponge to promote PCa progression by upregulating TGF-β-R2/SMAD signaling. Pang *et al* (27) reported that miR-373 expression is downregulated in PCa cell lines and tissues, which suppresses the TGF-β-R2/p-SMAD3 pathway to inhibit the invasion of PCa C4-2, PC3 and CWR22Rv1 cells (26). Overexpression of miR-373 decreases the invasion, migration and EMT potential of PCa cells (27). Thus, miR-373-3p may be used as a promising biomarker for PCa. In addition, the carcinogenic effect of miR-373-3p has been confirmed in several tumors. For example, miR-373 suppresses the progression, metastasis and inflammation of breast cancer by inhibiting NF-κB and the TGF-β/TGF-β-R2/SMAD pathway (54). Furthermore, miR-373 inhibits the invasion and peritoneal dissemination of pancreatic cancer cells by suppressing the EMT process (55). However, miR-373 acted as a carcinogen in testicular germ cell carcinoma by regulating p53/CDK (56). Thus, miR-373-3p has a dual function as a promoter or suppressor in different types of cancer. miRNAs are single-stranded non-coding RNAs that regulate gene expression through a conservative mechanism across metazoans (57). Furthermore, miR-373-3p directly targets TGF-β-R2 3'-UTR to regulate PCa cell proliferation and metastasis (26); thus, TGF-β-R2 is an important cancer driver (58,59). Downregulation of TGF-β-R2 inhibits the expression of SMAD-dependent metastasis-promoting genes and invasion (54). High expression of TGF-β-R2 enhances PCa cell proliferation by promoting p-SMAD2/3/c-MYC signaling (60). TGF-β-R2 is associated with NF-κB and TGF-β signals to drive the progression, EMT and metastasis of castration-resistant PCa (61).

In conclusion, the results of the present study demonstrated that SNHG16, miR-373-3p and TGF-β-R2 are important factors in PCa pathogenesis. SNHG16 promotes the proliferation, migration and invasion of PCa cell by sponging miR-373-3p to regulate the TGF-β-R2/SMAD pathway. Thus, targeting SNHG16 may be an effective strategy for the treatment of PCa.

The present study is not without limitations. First, although the expression levels of SNHG16, miR-373-3p and TGF-β-R2 were analyzed in RWPE1, DU-145, PC-3, 22Rv-1 and LNCaP cells, the contribution of SNHG16/miR-373-3p/TGF-β-R2

signaling to tumorigenesis was verified only in DU-145 cells. Thus, prospective studies will aim to analyze the role of SNHG16/miR-373-3p/TGF-β-R2 signaling in other PCa cell lines. Secondly, the present study failed to construct an animal model to verify the role of SNHG16 in PCa. Thus, additional animal experiments are required to determine whether SNHG16 acts as a ceRNA to regulate the miR-373-3p/TGF-β-R2 axis, and that it affects the biological functions of PCa cells.

**Acknowledgements**

Not applicable.

**Funding**

The present study was supported by the Natural Science Foundation of Fujian province (grant no. 2018J01220).

**Availability of data and materials**

All datasets used and/or analyzed during the present study are available from the corresponding author upon reasonable request.

**Authors' contributions**

WW and CL made substantial contributions to the conception and design of the present study. WW, CL, GL, QR, HL, NL and GC made substantial contributions to the acquisition, analysis and interpretation of the data. WW and CL confirm the authenticity of all the raw data. WW participated in drafting the initial manuscript, and CL critically revised the manuscript for important intellectual content. All authors have read and approved the final manuscript.

**Ethics approval and consent to participate**

The present study was approved by the Ethics Committee of Mindong Hospital Affiliated to Fujian Medical University [batch no. (2019) NingMin Medical Ethics approval no (0110-1)], and performed in accordance with the Declaration of Helsinki. Written informed consent was provided by all patients prior to the study start.

**Patient consent for publication**

Not applicable.

**Competing interests**

The authors declare that they have no competing interests.

**References**

1. Pishgar F, Ebrahimi H, Saeedi Moghaddam S, Fitzmaurice C and Amini E: Global, regional and national burden of prostate cancer, 1990 to 2015: Results from the global burden of Disease Study 2015. J Urol 199: 1224-1232, 2018.
2. Litwin MS and Tan HJ: The diagnosis and treatment of prostate cancer: A review. JAMA 317: 2532-2542, 2017.
3. Siegel RL, Miller KD and Jemal A: Cancer statistics, 2017. CA Cancer J Clin 67: 7-30, 2017.
4. Siegel RL, Miller KD and Jemal A: Cancer statistics, 2020. CA Cancer J Clin 70: 7-30, 2020.
5. Arora K and Barbieri CE: Molecular subtypes of prostate cancer. Curr Oncol Rep 20: 58, 2018.
6. Hua JT, Chen S and He HH: Landscape of noncoding RNA in prostate cancer. Trends Genet 35: 840-851, 2019.
7. Dragomir MP, Kopetz S, Ajani JA and Calin GA: Non-coding RNAs in GI cancers: From cancer hallmarks to clinical utility. Gut 69: 748-763, 2020.
8. Ponting CP, Oliver PL and Reik W: Evolution and functions of long noncoding RNAs. Cell 136: 629-641, 2009.
9. Lingadahalli S, Jadhao S, Sung YY, Chen M, Hu L, Chen X and Cheung E: Novel lncRNA LINC00844 regulates prostate cancer cell migration and invasion through AR signaling. Mol Cancer Res 16: 1865-1878, 2018.
10. Gu P, Chen X, Xie R, Han J, Xie W, Wang B, Dong W, Chen C, Yang M, Jiang J, *et al*: lncRNA HOXD-AS1 regulates proliferation and chemo-resistance of castration-resistant prostate cancer via recruiting WDR5. Mol Ther 25: 1959-1973, 2017.
11. Salameh A, Lee AK, Cardó-Vila M, Nunes DN, Efstathiou E, Staquicini FI, Dobroff AS, Marchiò S, Navone NM, Hosoya H, *et al*: PRUNE2 is a human prostate cancer suppressor regulated by the intronic long noncoding RNA PCA3. Proc Natl Acad Sci USA 112: 8403-8408, 2015.
12. Liao W and Zhang Y: MicroRNA-381 facilitates autophagy and apoptosis in prostate cancer cells via inhibiting the RELN-mediated PI3K/AKT/mTOR signaling pathway. Life Sci 254: 117672, 2020.
13. Bhatia V, Yadav A, Tiwari R, Nigam S, Goel S, Carskadon S, Gupta N, Goel A, Palanisamy N and Ateeq B: Epigenetic silencing of miRNA-338-5p and miRNA-421 drives SPINK1-positive prostate cancer. Clin Cancer Res 25: 2755-2768, 2019.
14. Lee YS and Dutta A: MicroRNAs in cancer. Annu Rev Pathol 4: 199-227, 2009.
15. Rupaimoole R and Slack FJ: MicroRNA therapeutics: Towards a new era for the management of cancer and other diseases. Nat Rev Drug Discov 16: 203-222, 2017.
16. He JH, Han ZP, Zou MX, Wang L, Lv YB, Zhou JB, Cao MR and Li YG: Analyzing the LncRNA, miRNA, and mRNA regulatory network in prostate cancer with bioinformatics software. J Comput Biol 25: 146-157, 2018.
17. Christensen LL, True K, Hamilton MP, Nielsen MM, Damas ND, Damgaard CK, Ongen H, Dermitzakis E, Bramsen JB, Pedersen JS, *et al*: SNHG16 is regulated by the Wnt pathway in colorectal cancer and affects genes involved in lipid metabolism. Mol Oncol 10: 1266-1282, 2016.
18. Zhu H, Zeng Y, Zhou CC and Ye W: SNHG16/miR-216-5p/ZEB1 signal pathway contributes to the tumorigenesis of cervical cancer cells. Arch Biochem Biophys 637: 1-8, 2018.
19. Zhong JH, Xiang X, Wang YY, Liu X, Qi LN, Luo CP, Wei WE, You XM, Ma L, Xiang BD, *et al*: The lncRNA SNHG16 affects prognosis in hepatocellular carcinoma by regulating p62 expression. J Cell Physiol 235: 1090-1102, 2020.
20. Zhou XY, Liu H, Ding ZB, Xi HP and Wang GW: lncRNA SNHG16 promotes glioma tumorigenicity through miR-373/EGFR axis by activating PI3K/AKT pathway. Genomics 112: 1021-1029, 2020.
21. Shao M, Yu Z and Zou J: LncRNA-SNHG16 silencing inhibits prostate carcinoma cell growth, downregulate GLUT1 expression and reduce glucose uptake. Cancer Manag Res 12: 1751-1757, 2020.
22. Tang Z, Xu Z, Zhu X and Zhang J: New insights into molecules and pathways of cancer metabolism and therapeutic implications. Cancer Commun (Lond) 41: 16-36, 2021.
23. Yang M and Wei W: SNHG16: A novel long-non coding RNA in human cancers. OncoTargets Ther 12: 11679-11690, 2019.
24. Zhao W, Fu H, Zhang S, Sun S and Liu Y: LncRNA SNHG16 drives proliferation, migration, and invasion of hemangioma endothelial cell through modulation of miR-520d-3p/STAT3 axis. Cancer Med 7: 3311-3320, 2018.
25. Albini A, Bruno A, Noonan DM and Mortara L: Contribution to tumor angiogenesis from innate immune cells within the tumor microenvironment: Implications for immunotherapy. Front Immunol 9: 527, 2018.
26. Qiu X, Zhu J, Sun Y, Fan K, Yang DR, Li G, Yang G and Chang C: TR4 nuclear receptor increases prostate cancer invasion via decreasing the miR-373-3p expression to alter TGFβR2/p-Smad3 signals. Oncotarget 6: 15397-15409, 2015.
27. Pang J, Dai L, Zhang C and Zhang Q: MiR-373 inhibits the epithelial-mesenchymal transition of prostatic cancer via targeting runt-related transcription factor 2. J Healthc Eng 2021: 6974225, 2021.

28. Lu Y, Li X, Zuo Y, Xu Q, Liu L, Wu H, Chen L, Zhang Y, Liu Y and Li Y: miR-373-3p inhibits epithelial-mesenchymal transition via regulation of TGFβR2 in choriocarcinoma. J Obstet Gynaecol Res 47: 2417-2432, 2021.
29. Wei F, Cao C, Xu X and Wang J: Diverse functions of miR-373 in cancer. J Transl Med 13: 162, 2015.
30. Weng J, Zhang H, Wang C, Liang J, Chen G, Li W, Tang H and Hou J: miR-373-3p targets DKK1 to promote EMT-induced metastasis via the Wnt/β-catenin pathway in tongue squamous cell carcinoma. BioMed Res Int 2017: 6010926, 2017.
31. Seol HS, Akiyama Y, Shimada S, Lee HJ, Kim TI, Chun SM, Singh SR and Jang SJ: Epigenetic silencing of microRNA-373 to epithelial-mesenchymal transition in non-small cell lung cancer through IRAK2 and LAMP1 axes. Cancer Lett 353: 232-241, 2014.
32. Zhu B and Kyprianou N: Transforming growth factor beta and prostate cancer. Cancer Treat Res 126: 157-173, 2005.
33. Zhao W, Zhu Q, Tan P, Ajibade A, Long T, Long W, Li Q, Liu P, Ning B, Wang HY, *et al*: Tgfbr2 inactivation facilitates cellular plasticity and development of Pten-null prostate cancer. J Mol Cell Biol 10: 316-330, 2018.
34. Ma G, Tang M, Wu Y, Xu X, Pan F and Xu R: LncRNAs and miRNAs: Potential biomarkers and therapeutic targets for prostate cancer. Am J Transl Res 8: 5141-5150, 2016.
35. Moris L, Cumberbatch MG, Van den Broeck T, Gandaglia G, Fossati N, Kelly B, Pal R, Briers E, Cornford P, De Santis M, *et al*: Benefits and risks of primary treatments for high-risk localized and locally advanced prostate cancer: An international multidisciplinary systematic review. Eur Urol 77: 614-627, 2020.
36. Maruyama T, Nishihara K, Umikawa M, Arasaki A, Nakasone T, Nimura F, Matayoshi A, Takei K, Nakachi S, Kariya KI, *et al*: MicroRNA-196a-5p is a potential prognostic marker of delayed lymph node metastasis in early-stage tongue squamous cell carcinoma. Oncol Lett 15: 2349-2363, 2018.
37. Prensner JR, Iyer MK, Sahu A, Asangani IA, Cao Q, Patel L, Vergara IA, Davicioni E, Erho N, Ghadessi M, *et al*: The long noncoding RNA SChLAP1 promotes aggressive prostate cancer and antagonizes the SWI/SNF complex. Nat Genet 45: 1392-1398, 2013.
38. Yu M, Ohira M, Li Y, Niizuma H, Oo ML, Zhu Y, Ozaki T, Isogai E, Nakamura Y, Koda T, *et al*: High expression of ncRAN, a novel non-coding RNA mapped to chromosome 17q25.1, is associated with poor prognosis in neuroblastoma. Int J Oncol 34: 931-938, 2009.
39. Lian D, Amin B, Du D and Yan W: Enhanced expression of the long non-coding RNA SNHG16 contributes to gastric cancer progression and metastasis. Cancer Biomark 21: 151-160, 2017.
40. Yang XS, Wang GX and Luo L: Long non-coding RNA SNHG16 promotes cell growth and metastasis in ovarian cancer. Eur Rev Med Pharmacol Sci 22: 616-622, 2018.
41. Xiao Y, Xiao T, Ou W, Wu Z, Wu J, Tang J, Tian B, Zhou Y, Su M and Wang W: LncRNA SNHG16 as a potential biomarker and therapeutic target in human cancers. Biomark Res 8: 41, 2020.
42. Qi P, Xu MD, Ni SJ, Shen XH, Wei P, Huang D, Tan C, Sheng WQ, Zhou XY and Du X: Down-regulation of ncRAN, a long non-coding RNA, contributes to colorectal cancer cell migration and invasion and predicts poor overall survival for colorectal cancer patients. Mol Carcinog 54: 742-750, 2015.
43. Xu F, Zha G, Wu Y, Cai W and Ao J: Overexpressing lncRNA SNHG16 inhibited HCC proliferation and chemoresistance by functionally sponging hsa-miR-93. OncoTargets Ther 11: 8855-8863, 2018.
44. Qi JC, Yang Z, Zhang YP, Lu BS, Yin YW, Liu KL, Xue WY, Qu CB and Li W: miR-20b-5p, TGFBR2, and E2F1 form a regulatory loop to participate in epithelial to mesenchymal transition in prostate cancer. Front Oncol 9: 1535, 2020.
45. Liu JJ, Zhang X and Wu XH: miR-93 promotes the growth and invasion of prostate cancer by upregulating its target genes TGFBR2, ITGB8, and LATS2. Mol Ther Oncolytics 11: 14-19, 2018.
46. Xu W, Zeng F, Li S, Li G, Lai X, Wang QJ and Deng F: Crosstalk of protein kinase C ε with Smad2/3 promotes tumor cell proliferation in prostate cancer cells by enhancing aerobic glycolysis. Cell Mol Life Sci 75: 4583-4598, 2018.
47. Yang F, Strand DW and Rowley DR: Fibroblast growth factor-2 mediates transforming growth factor-beta action in prostate cancer reactive stroma. Oncogene 27: 450-459, 2008.
48. Yang J, Song K, Krebs TL, Jackson MW and Danielpour D: Rb/E2F4 and Smad2/3 link survivin to TGF-beta-induced apoptosis and tumor progression. Oncogene 27: 5326-5338, 2008.
49. Waghray A, Schober M, Feroze F, Yao F, Virgin J and Chen YQ: Identification of differentially expressed genes by serial analysis of gene expression in human prostate cancer. Cancer Res 61: 4283-4286, 2001.
50. DuPree EL, Mazumder S and Almasan A: Genotoxic stress induces expression of E2F4, leading to its association with p130 in prostate carcinoma cells. Cancer Res 64: 4390-4393, 2004.
51. Littler S, Sloss O, Geary B, Pierce A, Whetton AD and Taylor SS: Oncogenic MYC amplifies mitotic perturbations. Open Biol 9: 190136, 2019.
52. Zhang R, Li P, Lv H, Li N, Ren S and Xu W: Exosomal SNHG16 secreted by CSCs promotes glioma development via TLR7. Stem Cell Res Ther 12: 349, 2021.
53. Bai S, Cao S, Jin L, Kobelski M, Schouest B, Wang X, Ungerleider N, Baddoo M, Zhang W, Corey E, *et al*: A positive role of c-Myc in regulating androgen receptor and its splice variants in prostate cancer. Oncogene 38: 4977-4989, 2019.
54. Keklikoglou I, Koerner C, Schmidt C, Zhang JD, Heckmann D, Shavinskaya A, Allgayer H, Gückel B, Fehm T, Schneeweiss A, *et al*: MicroRNA-520/373 family functions as a tumor suppressor in estrogen receptor negative breast cancer by targeting NF-κB and TGF-β signaling pathways. Oncogene 31: 4150-4163, 2012.
55. Nakata K, Ohuchida K, Mizumoto K, Aishima S, Oda Y, Nagai E and Tanaka M: Micro RNA-373 is down-regulated in pancreatic cancer and inhibits cancer cell invasion. Ann Surg Oncol 21 (Suppl 4): S564-S574, 2014.
56. Voorhoeve PM, le Sage C, Schrier M, Gillis AJ, Stoop H, Nagel R, Liu YP, van Duijse J, Drost J, Griekspoor A, *et al*: A genetic screen implicates miRNA-372 and miRNA-373 as oncogenes in testicular germ cell tumors. Cell 124: 1169-1181, 2006.
57. Bartel DP: Metazoan MicroRNAs. Cell 173: 20-51, 2018.
58. Nadauld LD, Garcia S, Natsoulis G, Bell JM, Miotke L, Hopmans ES, Xu H, Pai RK, Palm C, Regan JF, *et al*: Metastatic tumor evolution and organoid modeling implicate TGFBR2 as a cancer driver in diffuse gastric cancer. Genome Biol 15: 428, 2014.
59. Moon H, Ju HL, Chung SI, Cho KJ, Eun JW, Nam SW, Han KH, Calvisi DF and Ro SW: Transforming growth factor-β promotes liver tumorigenesis in mice via up-regulation of snail. Gastroenterology 153: 1378-1391.e6, 2017.
60. Ayub SG, Kaul D and Ayub T: An androgen-regulated miR-2909 modulates TGFβ signalling through AR/miR-2909 axis in prostate cancer. Gene 631: 1-9, 2017.
61. Pollard BS, Suckow MA, Wolter WR, Starr JM, Eidelman O, Dalgard CL, Kumar P, Battacharyya S, Srivastava M, Biswas R, *et al*: Digitoxin inhibits epithelial-to-mesenchymal-transition in hereditary castration resistant prostate cancer. Front Oncol 9: 630, 2019.